

MODELING AND ANALYSIS OF A SIX-PHASE INDUCTION MOTOR DRIVE WITH HARMONIC INJECTION FOR TORQUE-DENSITY IMPROVEMENT

ELVES SOUSA SILVA*, ISAAC SOARES DE FREITAS*, ITALO R. F. M. P. DA SILVA†, FABIANO SALVADORI*, CURSINO BRADÃO JACOBINA‡

*Department of Electrical Engineering
Federal University of Paraíba
João Pessoa, Paraíba, Brazil

†Department of Electrical Engineering
Federal Rural University of Pernambuco
Cabo de Santo Agostinho, Pernambuco, Brazil

‡Department of Electrical Engineering
Federal University of Campina Grande
Campina Grande, Paraíba, Brazil

Emails: elvessilva@hotmail.com, isaacfreitas@cear.ufpb.br, italo.roger@gmail.com, salvadori.fabiano@cear.ufpb.br, jacobina@dee.ufcg.edu.br

Abstract— In this paper is presented the modeling and analysis of a six-phase induction machine considering the space harmonic components. It is shown that the harmonic injection in phase voltages provides an increase in torque, therefore, improving the torque density of the drive system. It is presented the machine dynamical model, the steady state analysis and experimental results.

Keywords— Induction motor, Motor Drive, Six phase induction motor

Resumo— Neste artigo é apresentado o modelo de uma máquina de indução hexafásica considerando as harmônicas espaciais de fluxo (primeira, terceira e quinta). É demonstrado que a terceira e a quinta harmônica espacial de fluxo produz torque útil que se soma ao torque da componente fundamental de fluxo. Uma análise de regime permanente demonstra que excitando-se tais harmônicas espaciais de fluxo com harmônicas temporais de corrente a capacidade de produção de torque da máquina é aumentado. Resultados experimentais são incluídos e demonstram tal fato.

Palavras-chave— Máquinas hexafásicas, Acionamentos Elétricos, Máquinas de Indução

1 Introduction

Multi-phase machines present reduced torque pulsation, improved flux density and torque, reduced power switches ratings in the power converter of the drive system and additional degrees of freedom which can be used for extra fault tolerant capability and multi-machines drive [Toliyat et al. (1991a);Toliyat et al. (1991b); Levi et al. (2007)]. The multi-phase machine model with the space harmonics taken into consideration shown in [Fudeh and Ong (1983a); Fudeh and Ong (1983b); Fudeh and Ong (1983c)] demonstrates that, although for a three-phase winding, only the fundamental space flux produces dc torque, in a multi-phase winding the higher order space harmonics can also produce dc-torque. In Lyra and Lipo (2002) is presented a study for this capability in the six phase induction machine. In this paper a six-phase induction motor was modeled allowing for space harmonics and the steady state analysis was included. An experimental prototype was built and verified, which demonstrates the capability for increase in torque production with the harmonic injection.

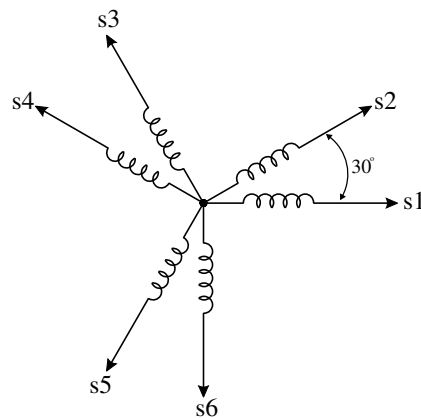


Figure 1: Magnetic axis of the stator phases.

2 MACHINE MODEL

By considering all harmonic components in the MMF distribution of an actual winding [Lipo (2017)] for determination of the machine inductances (self and mutual), as done in Fudeh and Ong (1983a), a general model can be evaluated for a M stator phases and N rotor phases induction machine. Such approach is used to evolve a general model for the five-phase induction machine in

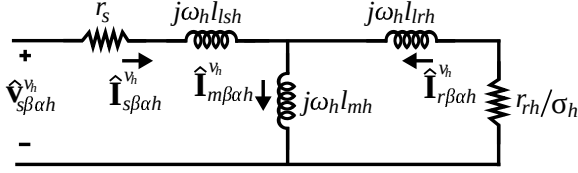


Figure 2: Steady state equivalent circuit for each *MMF* component

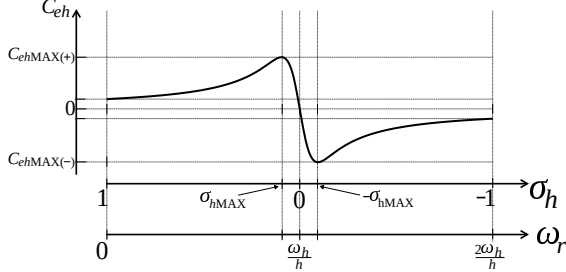


Figure 3: Steady state typical curves for each component model

Pereira et al. (2006). In this paper such approach is used for the six phase induction machine.

The six-phase induction machine under investigation in this paper is a cage rotor machine with a stator winding comprised by two sets of three-phase windings spatially shifted by an angle of $\alpha = 30^\circ$, as shown in Figure 1. From the general model, if only the fundamental, third and fifth harmonics of the *MMF* distribution are taken into consideration, then the following decoupled model for the six-phase induction machine is achieved ($h = 1, 3, 5$)

$$\hat{\lambda}_{s\beta\alpha h}^{g_h} = l_{sh} \hat{i}_{s\beta\alpha h}^{g_h} + l_{mh} \hat{i}_{r\beta\alpha h}^{g_h} \quad (1)$$

$$\hat{\lambda}_{r\beta\alpha h}^{g_h} = l_{rh} \hat{i}_{r\beta\alpha h}^{g_h} + l_{mh} \hat{i}_{s\beta\alpha h}^{g_h} \quad (2)$$

$$\hat{v}_{s\beta\alpha h}^{g_h} = r_s \hat{i}_{s\beta\alpha h}^{g_h} + j\omega_{g_h} \hat{\lambda}_{s\beta\alpha h}^{g_h} + \frac{d\hat{\lambda}_{s\beta\alpha h}^{g_h}}{dt} \quad (3)$$

$$\mathbf{0} = r_{rh} \hat{i}_{r\beta\alpha h}^{g_h} + j(\omega_{g_h} - h\omega_r) \hat{\lambda}_{r\beta\alpha h}^{g_h} + \frac{d\hat{\lambda}_{r\beta\alpha h}^{g_h}}{dt} \quad (4)$$

$$c_{eh} = phl_{mh} (i_{s\alpha h}^{g_h} i_{r\beta h}^{g_h} - i_{r\alpha h}^{g_h} i_{s\beta h}^{g_h}) \quad (5)$$

$$c_e = c_{e1} + c_{e3} + c_{e5}, \quad (6)$$

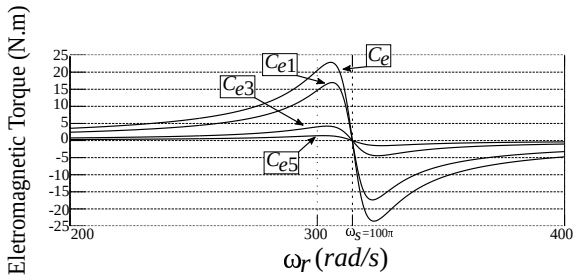


Figure 4: Steady state *Torque* \times *Speed* characteristics for voltage magnitudes chosen by (21) and $\omega_h = h\omega_s$

where $\hat{\lambda}_{s\beta\alpha h}^{g_h}$, $\hat{\lambda}_{r\beta\alpha h}^{g_h}$, $\hat{i}_{s\beta\alpha h}^{g_h}$, $\hat{i}_{r\beta\alpha h}^{g_h}$ and $\hat{v}_{s\beta\alpha h}^{g_h}$ are the stator and rotor linkage flux vectors, stator and rotor currents vectors and stator voltages vector; presented in a general reference frame. These vectors are complex quantities defined by

$$\hat{x}_{s\beta\alpha h}^{g_h} = \frac{1}{\sqrt{2}} (x_{s\beta h}^{g_h} + jx_{s\alpha h}^{g_h}) \quad (7)$$

$$\hat{x}_{r\beta\alpha h}^{g_h} = \frac{1}{\sqrt{2}} (x_{r\beta h}^{g_h} + jx_{r\alpha h}^{g_h}). \quad (8)$$

The real and imaginary components in (7) and (8) are transformed variables represented in a general reference frame, achieved from the stationary reference frame by

$$\begin{bmatrix} x_{s\alpha h}^{g_h} \\ x_{s\beta h}^{g_h} \end{bmatrix} = \mathbf{G}_h \begin{bmatrix} x_{s\alpha h}^s \\ x_{s\beta h}^s \end{bmatrix} \quad (9)$$

$$\begin{bmatrix} x_{r\alpha h}^{g_h} \\ x_{r\beta h}^{g_h} \end{bmatrix} = \mathbf{G}_h \begin{bmatrix} x_{r\alpha h}^s \\ x_{r\beta h}^s \end{bmatrix}, \quad (10)$$

where

$$\mathbf{G}_h = \begin{bmatrix} \sin(\delta_{g_h}) & \cos(\delta_{g_h}) \\ -\cos(\delta_{g_h}) & \sin(\delta_{g_h}) \end{bmatrix}. \quad (11)$$

In (11) the angle δ_{g_h} is the rotation angle from the stationary reference frame for each component, moreover, $\omega_{g_h} = \frac{d\delta_{g_h}}{dt}$.

The rotor variables in the stationary reference frame were obtained from the rotor natural reference frame by the Park transformation

$$\begin{bmatrix} x_{r\alpha h}^{s_h} \\ x_{r\beta h}^{s_h} \end{bmatrix} = \mathbf{P}_h \begin{bmatrix} x_{r\alpha h}^r \\ x_{r\beta h}^r \end{bmatrix} \quad (12)$$

$$\mathbf{P}_h = \begin{bmatrix} \sin(h\theta_r) & -\cos(h\theta_r) \\ \cos(h\theta_r) & \sin(h\theta_r) \end{bmatrix}, \quad (13)$$

where θ_r and $\omega_r = \frac{d\theta_r}{dt}$ are the electrical position and speed of the rotor, respectively.

The transformed stator variables in the natural reference frame were achieved from the actual machine phase variables by the following transformation

$$\begin{bmatrix} i_{s\alpha 1}^s \\ i_{s\beta 1}^s \\ i_{s\alpha 3}^s \\ i_{s\beta 3}^s \\ i_{s\alpha 5}^s \\ i_{s\beta 5}^s \end{bmatrix} = \mathbf{A}_s^T \begin{bmatrix} i_{s1} \\ i_{s2} \\ i_{s3} \\ i_{s4} \\ i_{s5} \\ i_{s6} \end{bmatrix}, \quad (14)$$

where,

$$\mathbf{A}_s = \frac{1}{\sqrt{3}} \begin{bmatrix} 1 & 0 & 1 & 0 & 1 & 0 \\ \frac{\sqrt{3}}{2} & \frac{1}{2} & 0 & 1 & -\frac{\sqrt{3}}{2} & \frac{1}{2} \\ -\frac{1}{2} & \frac{\sqrt{3}}{2} & 1 & 0 & -\frac{1}{2} & -\frac{\sqrt{3}}{2} \\ -\frac{\sqrt{3}}{2} & \frac{1}{2} & 0 & 1 & \frac{\sqrt{3}}{2} & \frac{1}{2} \\ -\frac{1}{2} & -\frac{\sqrt{3}}{2} & 1 & 0 & -\frac{1}{2} & \frac{\sqrt{3}}{2} \\ 0 & -1 & 0 & 1 & 0 & -1 \end{bmatrix}. \quad (15)$$

3 STEADY STATE ANALYSIS

In steady state each *MMF* model component in (1)-(5) is fed by a two-phase balanced voltage system. In the stationary reference frame, each voltage vector $\hat{\mathbf{v}}_{s\alpha\beta h}^{sh}$ is chosen as a sinusoidal balanced two-phase system with frequency ω_h .

If the machine model (1)-(5) is taken in the synchronous reference frame of each voltage, that means, choosing δ_{g_h} in (11) as

$$\delta_{g_h} = \omega_h t + \delta_{oh}, \quad (16)$$

the steady state conditions of (1)-(5) are dc-variables. These voltages reference frames will be indicated by $g_h \rightarrow v_h$ and the steady state of (1)-(5) becomes

$$\hat{\mathbf{v}}_{s\beta\alpha h}^{v_h} = r_s \hat{\mathbf{i}}_{s\beta\alpha h}^{v_h} + j\omega_h l_{lsh} \hat{\mathbf{i}}_{s\beta\alpha h}^{v_h} + j\omega_h l_{mh} \hat{\mathbf{i}}_{m\beta\alpha h}^{v_h} \quad (17)$$

$$\mathbf{0} = \frac{r_{rh}}{\sigma_h} \hat{\mathbf{i}}_{r\beta\alpha h}^{v_h} + j\omega_{hr} l_{lrh} \hat{\mathbf{i}}_{r\beta\alpha h}^{v_h} + j\omega_{hr} l_{mh} \hat{\mathbf{i}}_{m\beta\alpha h}^{v_h}, \quad (18)$$

where $\sigma_h = \frac{\omega_h - h\omega_r}{\omega_h}$, $l_{lsh} = l_{sh} - l_{mh}$, $l_{lrh} = l_{rh} - l_{mh}$, $\omega_{hr} = \omega_h - h\omega_r$ and $\hat{\mathbf{i}}_{m\beta\alpha h}^{v_h} = \hat{\mathbf{i}}_{s\beta\alpha h}^{v_h} + \hat{\mathbf{i}}_{r\beta\alpha h}^{v_h}$.

The steady state equivalent circuit for (17)-(18) is shown in Fig. 2.

From (17)-(18) the steady state torque (5) of each component can be found as

$$C_{eh} = \frac{2ph\omega_h l_{mk}^2}{\left(r_s \frac{r_{rh}}{\sigma_h} - \omega_h^2 \frac{l_{sh} l_{rh}}{\kappa_h}\right)^2 + \omega_h^2 \left(r_s l_{rh} + l_{sh} \frac{r_{rh}}{\sigma_h}\right)^2} \frac{r_{rh}}{\sigma_h} \left| \hat{\mathbf{v}}_{s\beta\alpha h}^{v_h} \right|^2, \quad (19)$$

where,

$$\kappa_h = \frac{l_{sh} l_{rh}}{l_{sh} l_{rh} - l_{mh}^2} = \frac{1}{1 - \frac{l_{mh}^2}{l_{sh} l_{rh}}}. \quad (20)$$

From (19) the typical *torque* \times *speed* characteristics is shown in Fig. 3 as a function of slip σ_h or rotor speed ω_r .

From Fig. 3, it can be seen that each space harmonic component behaves like a $p \times h$ poles machine. If the steady state frequency of each component is chosen to be $\omega_h = h\omega_s$, all space harmonic component has synchronous speed at the same rotor speed.

In Fig. 4 is shown a typical steady state *Torque* \times *Speed* characteristics for a synchronous frequency $\omega_s = 100\pi$, in which each frequency component being choose as $\omega_h = h\omega_s$ and each voltage magnitude is chosen as

$$\left| \hat{\mathbf{v}}_{s\beta\alpha h}^{v_h} \right| = \frac{\left| \hat{\mathbf{v}}_{s\beta\alpha 1}^{v_1} \right|}{h}. \quad (21)$$

Hence, the total torque is highly improved by the third and fifth harmonics injection in the voltage phases.

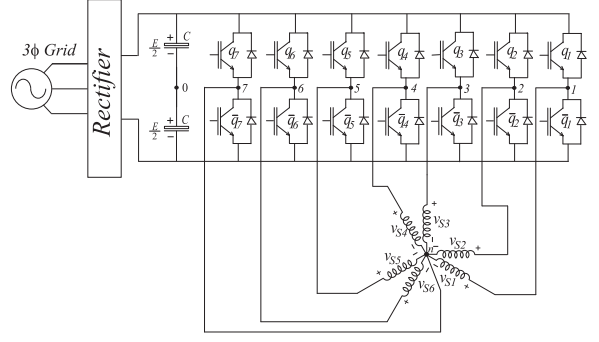


Figure 5: six-phase induction machine drive system

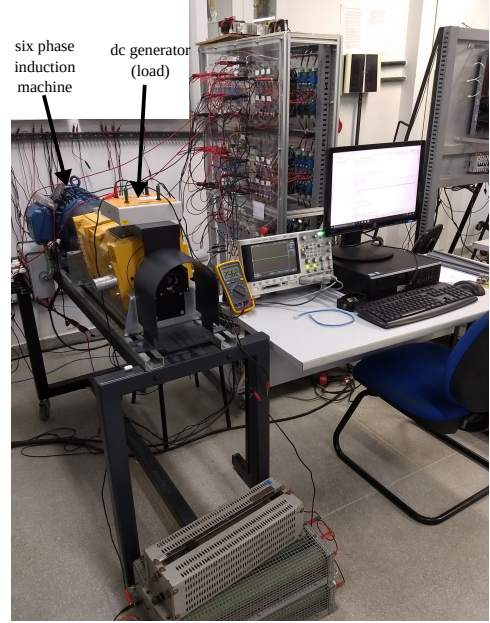


Figure 6: Experimental setup

4 EXPERIMENTAL RESULTS

To demonstrate the torque produced by each space harmonic component and the enhanced torque production in the six phase induction machine, a prototype machine and drive system was designed and built, as shown in Fig. 6. In order to be able to introduce a third harmonic voltage component, the six phase machine was driven by a seven leg power converter, as shown in Fig. 5

The dc-bus voltage of the power converter was adjusted to 400V and two tests were carried out.

The first test with no mechanical load, the machine started operation with a balanced voltage condition to the plane $\hat{\mathbf{v}}_{s\beta\alpha 1}^{g_1}$ with frequency $\omega_1 = 100\pi$ and zero voltages applied to the planes $\hat{\mathbf{v}}_{s\beta\alpha 3}^{g_3}$ and $\hat{\mathbf{v}}_{s\beta\alpha 5}^{g_5}$, see (3). After the machine reached steady state condition it was applied zero voltages to the planes $\hat{\mathbf{v}}_{s\beta\alpha 1}^{g_1}$ and $\hat{\mathbf{v}}_{s\beta\alpha 5}^{g_5}$ and a balanced voltage condition with frequency $\omega_3 = 300\pi$ was applied to the plane $\hat{\mathbf{v}}_{s\beta\alpha 3}^{g_3}$. In Fig. 7 is shown two of the machine phase voltages and phase currents along with the machine speed for

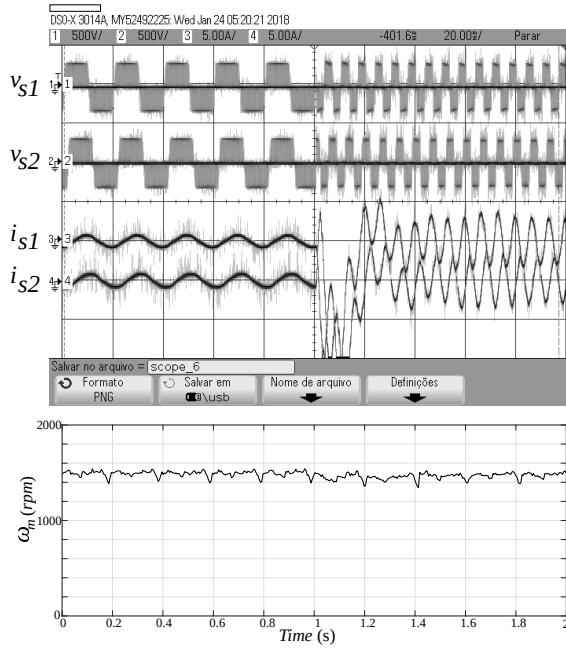


Figure 7: Experimental results for the first test conditions

this first test condition. It can be seen that the machine kept running unaffected after the fundamental space harmonic model has its voltage switched off and the third space harmonic model has its voltage switched on. This demonstrates the effectiveness of dc torque production by the third space harmonic component.

The second test with no mechanical load, the machine started operation with a balanced voltage condition to the plane $\hat{v}_{s\beta\alpha 1}^{g1}$ with frequency $\omega_s = 100\pi$ and zero voltages applied to the planes $\hat{v}_{s\beta\alpha 3}^{g3}$ and $\hat{v}_{s\beta\alpha 5}^{g5}$. After the machine reached steady state condition it was applied a high mechanical load condition (a dc generator was used in order to apply the mechanical load), after steady state is reached the third space harmonic plane had its voltage switched on with frequency $\omega_1 = 300\pi$ and magnitude at one third of the fundamental one. In Fig. 8 is shown two of the machine phase voltages and phase currents along with the machine speed, before and after the third harmonic injection for this second test condition. It can be seen that the machine speed increased after the third harmonic injection, which demonstrates the torque improvement.

Finally the machine was operated in ten different torque conditions, from no load to high load. The machine speed and torque were measured and a curve was fitted based on (19). These results are shown in in Fig. 9. In Fig. 9 is shown the torque *versus* speed characteristics for the machine fed with only the fundamental component (C_{e1}) and with the third harmonic injection ($C_{e1} + C_{e3}$). The actual experimental points are shown along with the fitted curves based on

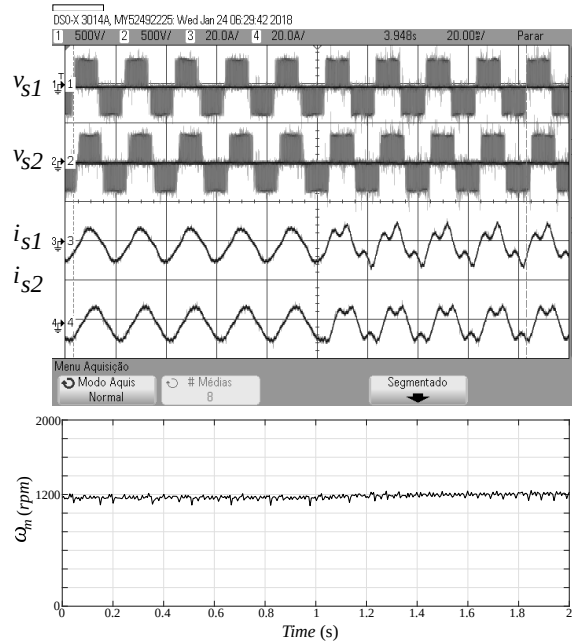


Figure 8: Experimental results for the second test conditions

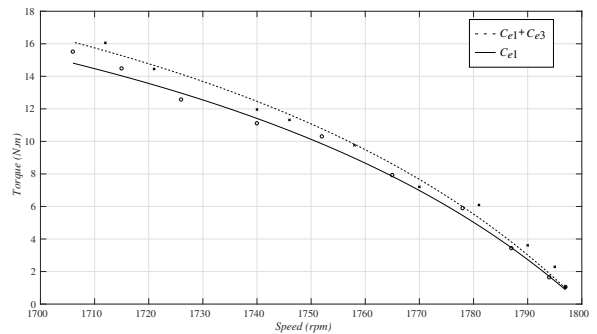


Figure 9: Experimental torque *versus* speed characteristics

(19). The increase in torque is close to 10% as can be seen in Fig. 10.

CONCLUSIONS

In this paper was shown the capability of the six-phase induction machine to produce torque with the fundamental and also with the third space harmonic. This capability was demonstrated by some preliminary results and can be effectively used to improve the torque production of such machine. This characteristic can be used by the drive system to enhance the torque density of the drive system.

Agradecimentos

The authors would like to thank the financial support provided by the National Council for Scientific and Technological Development (CNPq) and by the Coordination for the Improvement of

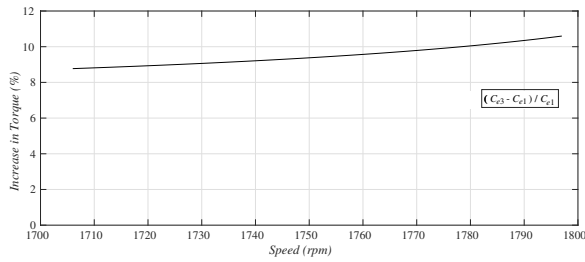


Figure 10: Increase in torque with the third harmonic injection compared to the fundamental one

Higher Education Personnel (CAPES).

References

- Fudeh, H. R. and Ong, C. M. (1983a). Modeling and analysis of induction machines containing space harmonics part i: Modeling and transformation, *IEEE Transactions on Power Apparatus and Systems* **PAS-102**(8): 2608–2615.
- Fudeh, H. R. and Ong, C. M. (1983b). Modeling and analysis of induction machines containing space harmonics part ii: Analysis of asynchronous and synchronous actions, *IEEE Transactions on Power Apparatus and Systems* **PAS-102**(8): 2616–2620.
- Fudeh, H. R. and Ong, C. M. (1983c). Modeling and analysis of induction machines containing space harmonics part iii: Three-phase cage rotor induction machines, *IEEE Transactions on Power Apparatus and Systems* **PAS-102**(8): 2621–2628.
- Levi, E., Bojoi, R., Profumo, F., Toliyat, H. A. and Williamson, S. (2007). Multiphase induction motor drives - a technology status review, *IET Electric Power Applications* **1**(4): 489–516.
- Lipo, T. A. (2017). *Introduction to AC Machine Design*, John Wiley & Sons, Inc., Hoboken, NJ, USA.
- Lyra, R. O. C. and Lipo, T. A. (2002). Torque density improvement in a six-phase induction motor with third harmonic current injection, *IEEE Transactions on Industry Applications* **38**(5): 1351–1360.
- Pereira, L. A., Scharlau, C. C., Pereira, L. F. A. and Haffner, J. F. (2006). General model of a five-phase induction machine allowing for harmonics in the air gap field, *IEEE Transactions on Energy Conversion* **21**(4): 891–899.
- Toliyat, H. A., Lipo, T. A. and White, J. C. (1991a). Analysis of a concentrated winding induction machine for adjustable speed drive

applications. i. motor analysis, *IEEE Transactions on Energy Conversion* **6**(4): 679–683.

Toliyat, H. A., Lipo, T. A. and White, J. C. (1991b). Analysis of a concentrated winding induction machine for adjustable speed drive applications. ii. motor design and performance, *IEEE Transactions on Energy Conversion* **6**(4): 684–692.